Title
Effective anisotropy gradient in pressure graded [Co/Pd] multilayers

Journal
Journal of Applied Physics, 117(6)

ISSN
0021-8979

Authors
Kirby, BJ
Greene, PK
Maranville, BB
et al.

Publication Date
2015-02-14

DOI
10.1063/1.4908140

Peer reviewed

Effective anisotropy gradient in pressure graded [Co/Pd] multilayers

B. J. Kirby,[1,a)] P. K. Greene,[2] B. B. Maranville,[1] J. E. Davies,[3] and Kai Liu[2]
[1]*Center for Neutron Research, NIST, Gaithersburg, Maryland 20899, USA*
[2]*Physics Department, University of California, Davis, California 95616, USA*
[3]*Advanced Technology Group, NVE Corporation, Eden Prarie, Minneapolis 55344, USA*

(Received 22 September 2014; accepted 1 February 2015; published online 12 February 2015)

We have used polarized neutron reflectometry to show that controlled variation of growth pressure during deposition of Co/Pd multilayers can be used to achieve a significant vertical gradient in the effective anisotropy. This gradient is strongly dependent on deposition order (low to high pressure or vice versa), and is accompanied by a corresponding gradient in saturation magnetization. These results demonstrate pressure-grading as an attractively simple technique for tailoring the anisotropy profile of magnetic media. © *2015 AIP Publishing LLC*. [http://dx.doi.org/10.1063/1.4908140]

I. INTRODUCTION

Exchanged coupled composites (ECC)—featuring a high anisotropy "hard" magnetic layer to serve as an anchor against thermal fluctuations exchange coupled to a low anisotropy "soft" magnetic layer to assist reversal—have been proposed as an optimized solution for simultaneously optimizing thermal stability and switching field distribution in magnetic media.[1,2] Suess took the concept further, proposing that a multilayer featuring a gradually varying anisotropy would constitute an ideally optimized ECC.[3] Since, such "graded anisotropy" magnetic multilayers have been studied both theoretically[4–7] and experimentally, including for multilayers where the anisotropy profile was controlled by varying layer thickness,[8] composition,[9] substrate temperature,[10] or ion irradiation.[11] Potentially, an attractively simple method for tailoring the anisotropy gradient of perpendicular anisotropy multilayers, such as Co/Pd and Co/Pt, is variation of deposition pressure during growth by sputtering. For these materials, increased sputtering pressure leads to increased disorder, e.g., rougher interfaces[12] and distinct grain boundary phase formation.[13] This in turn leads to smaller magnetic domains that reverse via more localized processes, resulting in films with increased coercivity, wider switching field distribution, and decreased saturation magnetization (M_S).[12–15] Vertically "pressure graded" Co/Pd has been studied with techniques, including magnetometry, scanning electron microscopy with polarization analysis, x-ray diffraction, and polarized neutron reflectometry (PNR),[15–17] but these studies have not addressed the nature of the anisotropy profile, i.e., the rate at which the magnetization at different depths in the multilayer changes with field. Where gradients in the magnetization profile have been reported,[16,17] a key issue is whether or not these gradients originate from depth variations in total moment (i.e., M_S), anisotropy, or both. To answer this question, we have performed PNR measurements of pressure-graded Co/Pd films over a hard-axis field range that spans positive saturation to negative reversal.

II. EXPERIMENT

Room temperature Ar^+ magnetron sputtering was used to deposit samples onto Si (100) substrates. The base pressure of the chamber was 1.2 μPa. A 20 nm Pd seed layer was sputtered at an argon pressure of 0.7 Pa, followed by $[Co(0.4\,nm)/Pd(0.6\,nm)]_{60}$ multilayers deposited under the following conditions and capped with 4.4 nm of Pd sputtered at 0.7 Pa:

- 3 Pressure 1 (3P1): bottom 30 bilayers sputtered at 0.7 Pa, the next 15 bilayers at 1.6 Pa, and the top 15 bilayers at 2.7 Pa.
- 3 Pressure 2 (3P2): bottom 15 bilayers sputtered at 2.7 Pa, the next 15 bilayers at 1.6 Pa, and the top 30 bilayers at 0.7 Pa.

The power was held constant at 20 W DC for the multilayer deposition, and the sputtering rate was calibrated at each pressure to ensure that the layer thicknesses remained constant. Detailed structural and magnetic characterizations of these two samples are discussed in Ref. 17. Figure 1 shows room temperature hysteresis loops for both samples measured with field perpendicular to plane (dashed lines) and parallel to plane (solid lines) as measured with vibrating sample magnetometry (VSM). For both samples, the perpendicular loop is more square and features a lower saturation

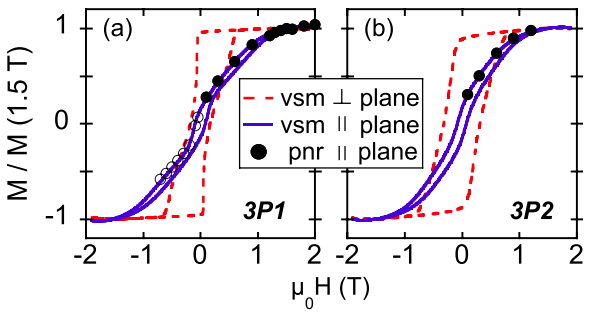

FIG. 1. Field-dependent magnetizations for 3P1 (a) and 3P2 (b). Lines correspond to VSM measurements, circles correspond PNR on NG-1 (open) and Asterix (closed).

[a)]Electronic mail: bkirby@nist.gov

field than does the in-plane loop, indicating a perpendicular easy axis.

Specular PNR is sensitive to the depth (z) dependent nuclear composition and magnetization (M) of thin films and multilayers. Detailed descriptions of the technique can be found in Refs. 18–20. Specifically, for neutrons with magnetic moment polarized either parallel (+) or anti-parallel (−) to a magnetic field H applied uniformly to the sample, the non-spin-flip wavevector transfer-dependent specular reflectivities $R(Q)^{++}$ and $R(Q)^{--}$ are dependent on the sample's nuclear scattering length density $\rho_N(z)$, and the component of the sample magnetization parallel to H, $M_{||}(z)$. It is straightforward to exactly calculate the reflectivity corresponding to a given profile,[18] thus $\rho(z)$ and $M_{||}(z)$ can be determined through model fitting of $R(Q)^{++}$ and $R(Q)^{--}$. While specular PNR is essentially insensitive to the component of the magnetization along the perpendicular-to-plane easy axis of our samples (the Halperin effect), the depth-dependent anisotropy can be probed by measuring the hard axis field dependence of $M_{||}(z)$.

With this in mind, room temperature non-spin-flip PNR measurements were conducted as a function of in-plane H using the NG-1 Reflectometer at the NIST Center for Neutron Research and Asterix at the Los Alamos Neutron Science Center.[21] First, consider sample 3P1 as it undergoes in-plane negative to positive magnetization reversal. An in-plane field of −3 T was applied to the sample offline, followed by PNR measurements conducted in progressively increasing positive in-plane field. Examples of the fitted data at 50 mT, 200 mT, and 600 mT are shown in Figure 2(a). Clear spin-dependent oscillations are observed, indicating sensitivity to $M_{||}(z)$. With increasing field, the magnitude of the spin-splitting increases, and the sense of the splitting changes sign, indicating sensitivity to the field-dependent evolution of the magnetic profile. Solid lines in Fig. 2(a) are fits to the data generated using the Refl1D software package.[22] The fits reproduce the data extremely well, and correspond to nuclear and magnetic depth profiles shown in Figs. 2(b) and 2(c). Although the multilayer structures of these samples are confirmed by x-ray diffraction,[17] the measured Q-range of the PNR data is well within the continuum limit for the multilayer ordering, meaning the measurements do not provide sensitivity to the individual Co and Pd layers. However, the effective spatial resolution is sufficient to provide information about the average properties of the individual pressure regions. Therefore, for simplicity, the neutron data are modeled in terms of a [Co/Pd] layer with constant ρ_N but depth-dependent $M_{||}$. Note that ρ_N of Co ($2.26 \times 10^{-4}\,\mathrm{nm}^{-2}$) is approximately half that of Pd ($4.01 \times 10^{-4}\,\mathrm{nm}^{-2}$).[23] Therefore, that good fits achieved by models with constant ρ_N for the [Co/Pd] indicates that the data are consistent with densities and relative thicknesses of the Co and Pd layers that are constant as a function of depth.[24]

The nuclear profile in Fig. 2(b) has features corresponding to the Si substrate, Pd seed layer, [Co/Pd] multilayer, and Pd cap, and provides reference for the field-dependent magnetic profiles shown in Fig. 2(c). The field-dependent magnetic profiles in 2(c) are highly non-uniform across the Co/Pd for all three fields. At 50 mT, the low pressure region of the Co/Pd retains a significant negative magnetization, while the higher pressure end has effectively zero magnetization. As field is increased to 200 mT, the magnetization of the low pressure region switches positive, while that of the high pressure regions remain near zero. Finally, as field is increased to 600 mT, the entire sample exhibits a significant positive in-plane magnetization. This shows that spins in different regions of the sample undergo magnetization reversal at different rates, and that 3P1 indeed exhibits a gradient in the effective anisotropy.

To further investigate the depth-dependent behavior, we used PNR to examine how spins in both samples relax in a progressively decreasing field after being saturated with a +3 T field along the hard axis. Selected magnetic profiles determined from these measurements are shown in Figure 3. Field-dependent $M_{||}(z)$ profiles for sample 3P1 in absolute units are shown in Fig. 3(a). The profile is highly non-uniform over the entire field range, featuring reduced magnetization near the surface, even at 3 T. A subsequent measurement at 10 T reveals a nonuniform profile similar to that measured at 3 T. This confirms that the sample is effectively saturated by 3 T, and that the sample exhibits a true gradient in M_S. To disentangle this M_S gradient from depth-dependent variations in the effective anisotropy, Fig. 3(b) shows the magnetization profiles normalized by the nominally saturating 3 T profile. This figure shows that with increasing deposition pressure, the in-plane magnetization decreases faster with decreasing in-plane field. Thus, this sample exhibits pronounced gradients in both M_S and effective anisotropy. The corresponding magnetic profiles for sample 3P2 are shown in Figs. 3(c) and 3(d). The depth and field-dependent magnetization variations are much suppressed compared to the 3P1 sample, both in absolute and normalized units, as disorder propagates vertically through the film depth.[17] The

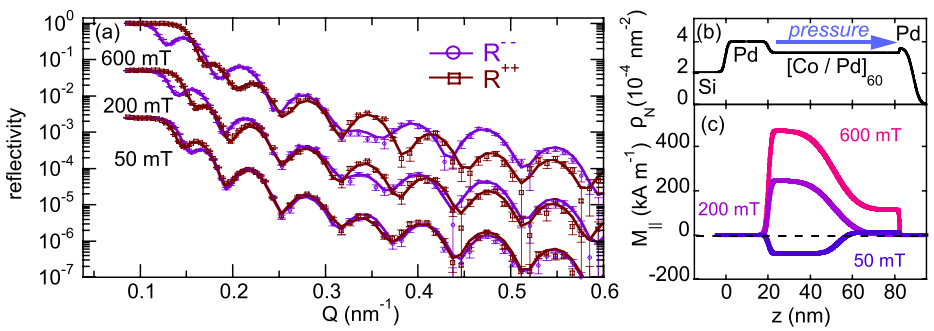

FIG. 2. (a) Example fitted reflectivities for sample 3P1 (low-to-high pressure) measured after saturating in a −3.0 T field. Data measured at different fields are separated vertically for clarity. Error bars correspond to ±1 standard deviation. Nuclear (b) and magnetic (c) depth profiles determined from the fits shown in (a).

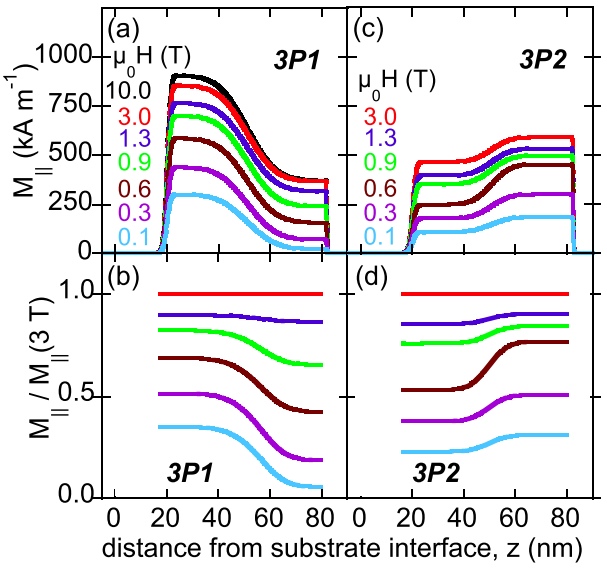

FIG. 3. Selected magnetization profiles for sample 3P1 (a) and (b) and 3P2 (c) and (d).

magnetic profiles can be compared to VSM results by integrating $M_{||}$ over all z, as shown by the solid points in Fig. 1. The normalized integrated values agree well with the corresponding VSM measurements, a strong confirmation of the model fitting.[25]

These field-dependent profiles can be put into a more familiar context by plotting $M(H)$ corresponding to different depths in the samples, as shown in Figures 4(a) and 4(b). Pressure-dependent variations in anisotropy are highlighted by plotting the ratio of the 0.7 Pa and 1.6 Pa region magnetizations to the 2.7 Pa magnetization, as shown in Figs. 4(c) and 4(d). For sample 3P1 at high fields near saturation, the ratio of the 0.7 Pa and 2.7 Pa magnetizations is relatively constant at about 2, but that value diverges dramatically below 1.5 T, indicative of the anisotropy gradient. Conversely, for sample 3P2, the magnetization ratio for 0.7 Pa and 2.7 Pa varies from only 1.3 at 3 T to 1.7 at 0.1 T. This demonstrates that reversing the pressure grading not only flattens the M_S profile but also flattens the effective anisotropy profile.

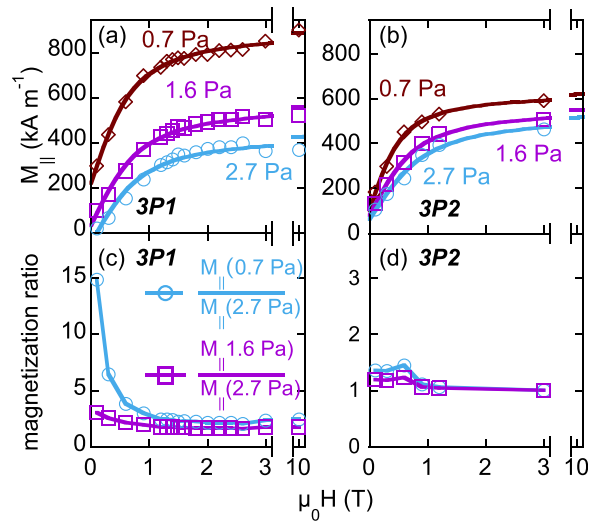

FIG. 4. Top: Field-dependent magnetizations of regions deposited at different pressures (depths) for sample 3P1 (a) and sample 3P2 (b). Bottom: Ratio of the 0.7 Pa region magnetization to the magnetization in the 2.7 Pa and 1.6 Pa regions, respectively, for samples 3P1 (c) and 3P2 (d).

III. DISCUSSION

In considering device applications that utilize the observed anisotropy gradient in pressure-graded Co/Pd, attention should be given to consequences of the accompanying M_S gradient. Some insight can be gained by considering a simple toy model that assumes perfect uniaxial anisotropy. To first order, the field associated with uniaxial anisotropy of energy density (anisotropy constant) K is linearly dependent on both K and M_S (Ref. 26)

$$H_A = \frac{2K}{\mu_0 M_S}. \tag{1}$$

In addition, M_S (i.e., the magnitude of the magnetization vector) has a linear effect on the Zeeman energy. For magnetization and easy axis separated by an angle ϕ, the Zeeman energy is[26]

$$W_z = \mu_0 H M_S \cos\left(\phi - \frac{\pi}{2}\right). \tag{2}$$

Thus, we identify two simple channels for M_S to linearly affect reversal behavior. To illustrate the role of the M_S gradient in pressure-graded Co/Pd, we have used the OOMMF micromagnetic software package[27] to simulate easy-axis hysteresis loops for three different "pillars" of spins, all with the same *average* anisotropy constant and M_S, but with different *distributions* of K and M_S. Each pillar consists of a $10 \times 10 \times 64$ nm array of 1 nm^3 spins, with an exchange constant of $A = 1.78$ pJ m^{-1},[28] average $K = 710$ kJ m^{-3},[28] and average $M_S = 629$ kA m^{-1} (i.e., the average value determined from PNR). Cartoon depictions of the three spin structures considered are shown in Figure 5(a):

- constant K (710 kJ m^{-3}) with constant M_S (629 kA m^{-1}),
- 40% graded K (500–1200 kJ m^{-3}) with constant M_S (629 kA m^{-1}),

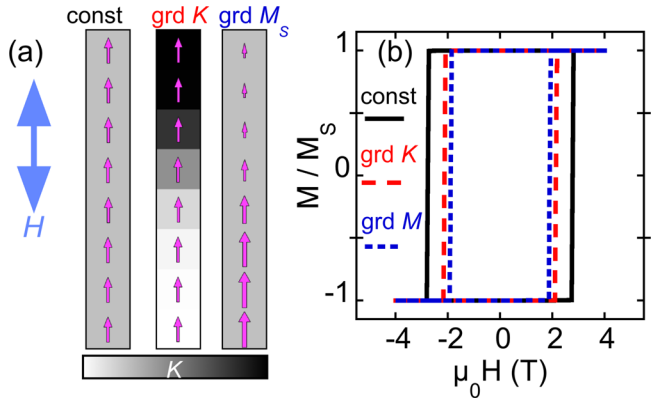

FIG. 5. (a) Depiction of spin structures used for micromagnetic simulations. Magnitude of M_S is depicted by arrow size, while magnitude of K is depicted by grayscale. (b) Simulated hysteresis loops for the three pillars shown in (a).

- constant K (710 kJ m^{-3}) with a 40% graded M_S (370–900 kA m^{-1}, i.e., the M_S profile shown for Fig. 3(a)).

Figure 5(b) shows simulated hysteresis loops for H along the long (easy) axes of the pillars. In this example, a 40% gradient in K results in a 13% reduction in coercive field as compared to the constant K, constant M_S pillar, while a 40% gradient in M_S alone leads a comparable 19% decrease. Therefore, the observed M_S gradient should contribute towards the desired reduction in switching field. However, it is not clear that such a M_S gradient yields a *net* benefit for graded media. Sophisticated micromagnetic simulations of bilayer ECC have shown that increasing the soft layer M_S with respect to that of the hard layer indeed reduces the switching field, but at the cost of decreased thermal stability,[3,29] with a uniform M_S profile corresponding to maximum stability for a given value of switching field.[30]

IV. CONCLUSION

In summary, we have explicitly demonstrated that a simple technique of varying pressure during sputtering can be used to create magnetic multilayers exhibiting a pronounced vertical gradient in the effective anisotropy, and that this anisotropy gradient depends strongly on the deposition order. Additionally, we find that pressure grading leads to a pronounced gradient in M_S that likely contributes to the coercivity reduction, but at the cost of reducing the thermal stability.

ACKNOWLEDGMENTS

Support from the NSF Materials World Network program (DMR-1008791) is gratefully acknowledged. We are extremely grateful to M. R. Fitzsimmons of Los Alamos National Laboratory for assistance with Asterix, as well Randy K. Dumas of Gothenburg University and P. A. Kienzle of NIST for valuable discussions regarding model fitting.

[1]R. H. Victora and X. Shen, IEEE Trans. Magn. **41**, 537 (2005).
[2]J. P. Wang, W. K. Shen, and J. M. Bai, IEEE Trans. Magn. **41**, 3181 (2005).
[3]D. Suess, Appl. Phys. Lett. **89**, 113105 (2006).
[4]G. T. Zimanyi, J. Appl. Phys. **103**, 07F543 (2008).
[5]D. Suess, J. Fidler, G. Zimanyi, T. Schrefl, and P. Visscher, Appl. Phys. Lett. **92**, 173111 (2008).
[6]R. Skomski, T. A. George, and D. J. Sellmyer, J. Appl. Phys. **103**, 07F531 (2008).
[7]D. Suess, J. Lee, J. Fidler, and T. Schrefl, J. Magn. Magn. Mater. **321**, 545 (2009).
[8]B. J. Kirby, J. E. Davies, K. Liu, S. M. Watson, G. T. Zimany, R. D. Shull, P. A. Kienzle, and J. A. Borchers, Phys. Rev. B **81**, 100405 (2010).
[9]R. K. Dumas, Y. Fang, B. J. Kirby, C. Zha, V. Bonanni, J. Nogues, and J. Åkerman, Phys. Rev. B **84**, 054434 (2011).
[10]J. Zhang, Z. Sun, J. Sun, S. Kang, G. H. S. Yu, S. Yan, L. Mei, and D. Li, Appl. Phys. Lett. **102**, 152407 (2013).
[11]P. K. Greene, J. Osten, K. Lenz, J. Fassbender, C. Jenkins, E. Arenholz, T. Endo, N. Iwata, and K. Liu, Appl. Phys. Lett. **105**, 072401 (2014).
[12]M. S. Pierce, C. R. Buechler, L. B. Sorensen, S. D. Kevan, E. A. Jagla, J. M. Deutsch, T. Mai, O. Narayan, J. E. Davies, K. Liu, G. T. Zimanyi, H. G. Katzgraber, O. Hellwig, E. E. Fullerton, P. Fischer, and J. B. Kortright, Phys. Rev. B **75**, 144406 (2007).
[13]M. S. Pierce, J. E. Davies, J. J. Turner, K. Chesnel, E. E. Fullerton, J. Nam, R. Hailstone, S. D. Kevan, J. B. Kortright, K. Liu, L. B. Sorensen, B. R. York, and O. Hellwig, Phys. Rev. B **87**, 184428 (2013).
[14]M. S. Pierce, C. R. Buechler, L. B. Sorensen, J. J. Turner, S. D. Kevan, E. A. Jagla, J. M. Deutsch, T. Mai, O. Narayan, J. E. Davies, K. Liu, J. H. Dunn, K. M. Chesnel, J. B. Kortright, O. Hellwig, and E. E. Fullerton, Phys. Rev. Lett. **94**, 017202 (2005).
[15]J. E. Davies, P. Morrow, C. L. Dennis, J. W. Lau, B. McMorran, A. Cochran, J. Unguris, R. K. Dumas, P. Greene, and K. Liu, J. Appl. Phys. **109**, 07B909 (2011).
[16]B. J. Kirby, S. M. Watson, J. E. Davies, G. T. Zimanyi, K. Liu, R. D. Shull, and J. A. Borchers, J. Appl. Phys. **105**, 07C929 (2009).
[17]P. K. Greene, B. J. Kirby, J. W. Lau, J. A. Borchers, M. R. Fitzsimmons, and K. Liu, Appl. Phys. Lett. **104**, 152401 (2014).
[18]C. F. Majkrzak, K. V. O'Donovan, and N. F. Berk, in *Neutron Scattering From Magnetic Materials*, edited by T. Chatterji (Elsevier Science, New York, 2005).
[19]C. F. Majkrzak, Physica B **221**, 342 (1996).
[20]M. R. Fitzsimmons and I. K. Schuller, J. Magn. Magn. Mater. **350**, 199 (2014).
[21]Spin-flip scattering is not expected, as it arises from the in-plane component of the magnetization perpendicular to H. Spin analysis at selected fields confirms the absence of spin-flip scattering.
[22]B. J. Kirby, P. A. Kienzle, B. B. Maranville, N. F. Berk, J. Krycka, F. Heinrich, and C. F. Majkrzak, Curr. Opin. Colloids Interface Sci. **17**, 44 (2012).
[23]M. R. Fitzsimmons and C. F. Majkrzak, in *Modern Techniques for Characterizing Magnetic Materials*, edited by Z. Zhu (Kluwer, New York, 2005).
[24]See supplementary material at http://dx.doi.org/10.1063/1.4908140 for additional details about the PNR measurements and interpretation.
[25]We note that when comparing in absolute units, PNR systematically gives magnetization values approximately 6% higher than that determined from VSM for 3P1, and approximately 4% lower for 3P2. This discrepancy does not affect the primary conclusions of this work.
[26]S. Chikazumi, in *Physics of Ferromagnetism*, 2nd ed., edited by J. Birman, S. F. Edwards, R. Friend, C. H. Llewellyn Smith, M. Rees, D. Sherrington, and G. Veneziano (Oxford University Press, Oxford, 1997), Chap. 12, p. 264.
[27]M. J. Donahue and D. G. Porter, in *OOMMF User's Guide, Version 1.0*, 2nd ed. (National Institute of Standards and Technology, Oxford, 1999), available at http://math.nist.gov/oommf/oommf_cites.html.
[28]P. Manchanda, R. Skomski, P. K. Sahota, M. Franchin, and H. Fanghor, J. Appl. Phys. **111**, 07C724 (2012).
[29]H. Kronmuller and D. Goll, Physica B **319**, 122 (2002).
[30]D. Suess, J. Magn. Magn. Mater. **308**, 183 (2007).